

# Vertical Axis Wind Turbine Performance Prediction, High and Low Fidelity Analysis

Franklyn Kanyako  
Masdar Institute of Science and Technology  
[fkanyako@masdar.ac.ae](mailto:fkanyako@masdar.ac.ae)

Isam Janajreh  
Masdar Institute of Science and Technology  
[ijanjreh@masdar.ac.ae](mailto:ijanjreh@masdar.ac.ae)

## Abstract

Vertical axis wind turbines have potential advantages for small domestic applications, as they can be effectively used in urban areas where wind is intermittently unsteady and turbulent. This work highlights the progress made in the development of aerodynamic models for predicting the performance of straight-bladed, fixed-pitch vertical axis wind turbine blade profiles. An improved low-fidelity blade element momentum algorithm using a hybrid database is built to investigate the solidity of the turbine, by analyzing the effect of blade chord, radius, and number blades at different tip speed ratios. This is followed by a 2-D numerical investigation to compare the performance prediction capability of the CFD and mathematical model. Both high- and low-fidelity analyses have shown minimum/negative performance at low tip speed ratio, indicating the general inability of the fixed pitch vertical axis turbine to self-start. The CFD analysis, although is computationally intensive, has shown better performance than the analytical solution and also captures important flow features, such as vortex shedding among other detailed flow field features.

## Introduction

The development of wind turbine technologies has allowed wind energy to perform a relevant step forward in local production of clean electric power inside the built environment. The present technical design relies exclusively on horizontal axis turbines and is not yet adequate to develop reliable wind energy converters, particularly for conditions corresponding to low wind speeds and/or urban areas. This has renewed interest in vertical axis wind turbines (VAWT), like the Darrieus turbine, which appear to be particularly promising for such conditions. These VAWTs can be used to power remote or off-grid applications such as homes, farms, refuges, or beacons. Intermediate-sized wind power systems (100 kW to 250 kW) can power a village or a cluster of small enterprises and can be grid-connected or off-grid. They can be coupled with diesel generators, batteries and other distributed energy sources for remote use where there is no access to the grid. However, the disadvantages of VAWTs stem from the fact that there is cyclical variation in the angle of attack on the aerofoils as the rotor rotates. As a result, optimal loading cannot be sustained for all azimuthal angles, leading to inherently low aerodynamic efficiency compared to horizontal axis wind turbines (HAWT)[1]. The rotation of the turbine in a 3-D environment leads to

several flow phenomena such as dynamic stall, flow separation, and flow wake deformation, making the aerodynamic analysis and performance prediction of the Darrieus wind turbine very difficult. Various computational models exist, each with their own strengths and weaknesses that attempt to accurately predict the performance of a wind turbine. Being able to numerically predict wind turbine performance offers a possibility to reduce the expensive and exhaustive wind tunnel and field experimental tests. The major benefit is that computational studies are more economical, versatile, and higher resolution than costly experiments.

### **Computational Models for VAWT**

Despite the complexity of the aerodynamic behavior of the Darrieus VAWT, several mathematical models, based on theories, have been prescribed for the performance prediction and design of a Darrieus VAWT. According to survey of aerodynamics models used for prediction of VAWT performance conducted by [1] and [2], the most studied and validated models can be broadly classified into three categories: momentum models, vortex models, and computational fluid dynamics (CFD).

The momentum model combines momentum theory with blade element theory [3]. It studies the behavior of air flow on the blades and its forces. They can be further divided into single stream tube, multiple stream tube, and double-multiple stream tube models. In the single stream tube model first developed by Templin for VAWT [4], the turbine is placed inside a single stream tube and blade revolution is translated in an actuator disk. The effects of the stream tube outside are assumed negligible, and the wind speed in the upstream and downstream sides of the turbine are assumed to be constant. This model suffers from performance accuracy prediction, due to the many assumptions, and usually gives higher prediction values.

The multiple stream tube model developed by Strickland [5] is a variation of the single stream tube model, where the single stream tube is divided into several parallel adjacent stream tubes that are independent from each other and have their own undisrupted wake and induced velocities. Several modifications/corrections have been incorporated to this model where the drag forces, aerofoil geometry, curvature flow, etc. were added; while it relatively provides better accuracy than single stream, it still lacks experimental validation. The double multiple stream tube (DMS) model is a variation of the multiple stream tube model, where the actuator disc is divided in two half cycles in tandem, representing the upstream and downstream sides of the rotor. This model was presented by Paraschivoiu [6].

Vortex models are basically potential flow models based on the calculation of the velocity field about the turbine through the influence of vorticity in the wake of the blades. The turbine blades are represented by bound or lifting-line vortices whose strengths are determined using airfoil coefficient datasets and calculated relative flow velocity and angle of attack. Larsen [7] first introduced the idea of the vortex model for a single blade element of a VAWT. He used the vortex model for the performance prediction of a cyclogiro windmill. The model is 2D, but if the vortex trailing from the rotor blade tips is considered, it may be

said that it is not strictly 2-D. However, in his model, angle of attack is assumed to be small; as a result, the stall effect is neglected. In 1979, Strickland et al. [8] presented an extension of the vortex model, which is 3-D, and the aerodynamic stall is incorporated into the model. They presented the experimental results for a series of two-dimensional rotor configurations. Their calculated values show good correlation with the experimental results for the instantaneous blade forces and the near wake flow behind the rotor. Strickland et al. [8] made improvements on the prior vortex model. The latest model is termed as the dynamic vortex model, since it includes the dynamic effects. The improvements over the prior model are that it includes the dynamic stall effect, pitching circulation, and added mass effect. The main disadvantage of vortex model is that it takes too much computation time. Furthermore, this model still relies on significant simplifications, like potential flow is assumed in the wake and the effect of viscosity in the blade aerodynamics is included through empirical force coefficients [9].

Computational fluid dynamics (CFD) is widely employed for VAWT performance analysis. It solves the Reynolds Averaged Navier-Stokes equation or the more advanced and costly direct numerical simulation, large eddy simulation, and detached eddy simulation (DES). Ivan Dobrev et al. [10] conducted high fidelity simulation to explore the possibility of using the 3-D Navier-Stokes solver DES solver/k-w model, and particle image velocimetry for experimental validation. The comparison of wake and shedding vorticity with experiments shows that the 3-D/k-w modeling gives results were quite similar to phase averaged velocity. The power coefficient measured was very close to the experiment result, confirming the capability of DES model to accurately capture the turbulent detached flow. Mohamed [11] carried out aerodynamic investigation for 20 different airfoils using 2-D unsteady Reynolds averaged Navier Stokes (RANS) simulation. He found the S-1046 profile for H-Darrieus rotor very promising for wind energy generation, in particular in urban areas compared to symmetric airfoils. Many other studies have been done using RANS [12-14]; however, CFD is computationally intensive as the aerodynamic performance of the turbine is a function of instantaneous forces and moment coefficient.

The objective of this study is to investigate some of the most significant parameters that affect the turbine performance, such as, turbine solidity, number of blades, airfoil selection, and turbine aspect ratio (H/D). This paper focuses on understanding the importance of these factors, specifically the first three ones, to find the best configuration of H-Darrieus turbines. This investigation is carried out by using double multiple stream model with a hybrid database of lift and drag coefficient prediction methodology from  $-180^{\circ}$  to  $180^{\circ}$  developed by Castelli et al. [15]. The result is compared with numerical simulation using unsteady Reynolds averaged Navier-Stokes solver.

## Aerodynamics Analysis of H-Darrieus VAWT

### DMST Model

For the low fidelity analysis, the DMST developed by Paraschivoiu is adapted to an H-Darrieus based on the these assumptions: unlike for the Troposkien/egg shaped Darrieus turbine used by Paraschivoi, it has been assumed no vertical variation of the induced velocity as straight vertical blade is subjected to the same flow velocity along its length. Therefore, the angle  $\delta$  that lies between the normal element to the blade element and horizontal XY plane is equated to zero ( $\delta = 0$ ). b) It is assumed fixed pitch VAWT; therefore, using symmetric airfoil section, the chord line is tangent to the circle of rotation (or blade flight path),  $\alpha_0 = 0$ .

The aerodynamic characteristics of straight blade Darrieus type VAWT are shown in Figure 1. The relative velocity component ( $V_R$ ) can be obtained from the cordial velocity component and normal velocity component as follows:

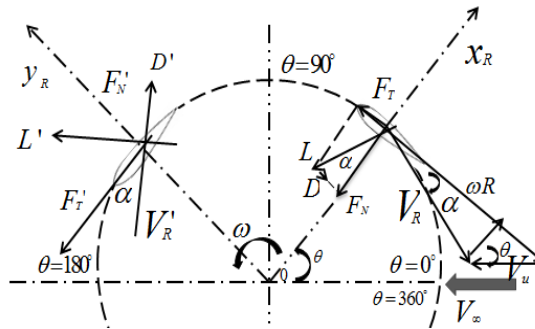


Figure 1. Flow velocities of straight-bladed Darrieus rotor

$$V_R = \sqrt{(V_u^2 [(X - \sin \theta)^2 + (\cos \theta)^2])} \quad (1)$$

where  $V_u$  is the induced velocity, defined as the axial flow velocity through the rotor,  $\theta$  is the azimuth angle and  $X$  is the local tip speed ratio defined as

$$X = \frac{\omega R}{V_u} \quad (2)$$

where  $\omega$  the turbine's angular speed and  $R$  is the rotor radius. The solidity represents the fraction of the frontal swept area of the wind turbine that is covered by the blades, defined as

$$\sigma = \frac{Nc}{R} \quad (3)$$

It is a function of the number of blades  $N$ , the chord length of the blades  $c$ , and the radius of the rotor  $R$ . From the geometry in Figure 1, the expression for the local angle of attack may be derived as

$$\alpha = \sin^{-1} \left[ \frac{\cos \theta}{\sqrt{(X - \sin \theta)^2 + \cos^2 \theta}} \right] \quad (4)$$

The normal and tangential force coefficients can be expressed as

$$C_n = C_L \cos \alpha + C_D \sin \alpha \quad (5)$$

$$C_t = C_L \sin \alpha + C_D \cos \alpha \quad (6)$$

where  $C_L$  is the lift coefficient and  $C_D$  is the drag coefficient for angle of attack  $\alpha$ . Then the normal and tangential forces for single blade at a single azimuthal location are

$$F_N = \frac{1}{2} \rho V_R^2 (hc) C_n \quad (7)$$

$$F_T = \frac{1}{2} \rho V_R^2 (hc) C_t \quad (8)$$

where  $h$  is the blade height and  $c$  is the blade chord length. Referring to Figure 1, the instantaneous thrust force which is the force of the wind on the turbine experienced by one blade element in the direction of the air flow is written as

$$T_i = \frac{1}{2} \rho V_R^2 (hc) (C_n \sin \theta - C_t \cos \theta) \quad (9)$$

This is because the tangential force component drives the rotation of the wind turbine and produces the torque necessary to generate electricity. The instantaneous torque or the torque by a single blade at a single azimuthal location is

$$Q_i = F_T R \quad (10)$$

Substituting equation 7 into 9 yields

$$Q_i = \frac{1}{2} \rho V_R^2 (hc) C_t R \quad (11)$$

Figure 2 presents the DMS model diagram. The actuator disc is divided into two actuator discs, each with its own induced velocity. The induced velocity decreases along the axial stream tube direction, so the induced velocity in the upstream  $V_{aui}$  is less than the undisturbed wind speed  $V_{\infty i}$  that arrives to the stream tube. Between the upstream and the downstream, there is an equilibrium induced velocity  $V_{ei}$  that is less than the  $V_{aui}$ .

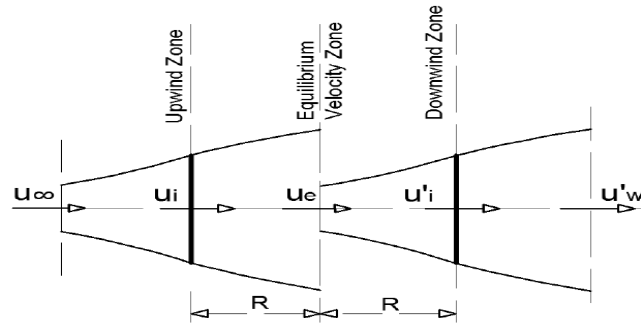


Figure 2. 2-D Schematic of the DMST model [16]

The induced velocity in the downstream  $V_{ad}$  is less than  $V_{ei}$ . So for the induced velocity in the upstream  $V_{au}$  one gets

$$V_{au} = V_{ei} U_{us} \quad (12)$$

where  $U_{us}$  is the interference factor for the upstream which is less than 1 and is given by

$$U_{us} = \frac{V_{au}}{V_{ei}} \quad (13)$$

The induced velocity in the midstream  $V_e$  is influenced by the wake velocity of the upstream, which is given by

$$V_e = V_{ei} \left( 2 \frac{V_{au}}{V_{ei}} - 1 \right) = V_{ei} (2U_{us} - 1) \quad (14)$$

The induced velocity in the downstream  $V_{ad}$  is given by

$$V_{ad} = U_{ds} V_e = U_{ds} (2U_{us} - 1) V_{ei} \quad (15)$$

where  $U_{ds}$  is the interference factor for the downstream. The  $U_{ds}$  is given by

$$U_{ds} = \frac{V_{ad}}{V_e} \quad (16)$$

As it can be seen, the aerodynamic behavior of the blades in the upstream side of the wind turbine will influence the induced velocity on the blades in the mid- and downstream regions. The undisturbed wind velocity  $V_{ei}$  is defined by the wind velocity profile and typically increases along the wind turbine height according to a given local atmospheric boundary layer velocity profile.

By applying the DMS model with the VAWT performance equations presented previously, it is possible to predict turbine performance. The torque and power coefficient are found by integrating the aerodynamic behaviors of the several stream tubes. The iterative procedure used in the DMST analysis is shown in Figure 3. For the whole process, 36 stream tubes had been used, i.e., evaluating the wind conditions at blade positions in  $5^\circ$  increments, no

significant difference was observed with increase in the number of stream tubes. The induction factors  $a_u$  and  $a_d$  are calculated for upstream, the mid- as well as downstream tubes of the turbine, respectively.

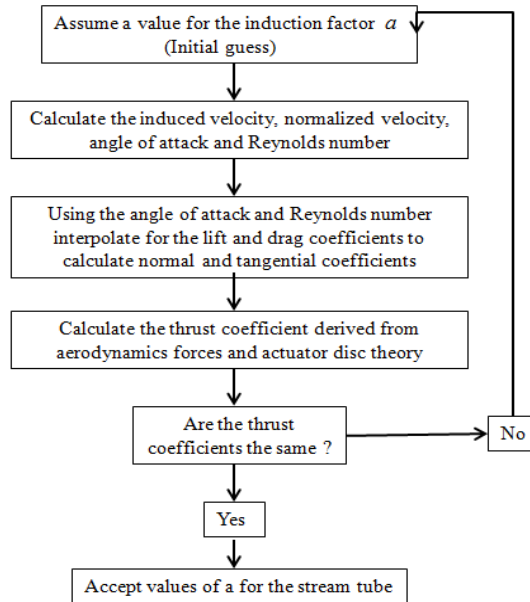


Figure 3. Iterative procedure used to calculate the flow velocity in DMST model

### ***CFD Model***

The 2-D wind turbine model has been created in GAMBIT meshing software. The mesh and boundary conditions are shown in Figure 4, in which the interior domain containing the wind turbine blades was considered as the moving mesh, while the outer domain was stationary. An unstructured grid has been chosen for the moving and structured grid for the stationary domain. An interface was set between the interior sliding and outer stationary domain. The mesh on both sides of the interface has approximately the same characteristic cell size, rendering the simulation more accurately and with faster convergence. The interior sliding domain rotated with a prescribed rotational velocity ( $\omega$ ). The inlet boundary was placed 3D upstream the outlet placed at 6D downstream. The domain around the airfoil should be wide enough to allow the vorticity and dynamic stall to fully develop. For both static and sliding models, the inlet boundary condition was velocity inlet. The upper and lower boundaries were supposed as symmetry, meaning zero normal gradients of pressure and velocity. The exit boundary is set as pressure outlet, with the gauge pressure set to zero gauge or atmospheric.

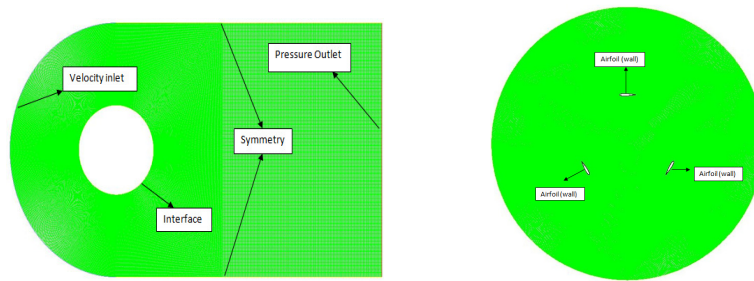


Figure 4. Boundary condition and rotor sub-grid mesh for 3-bladed VAWT

A boundary layer has been placed on the blade profile as shown in Figure 5, in order to capture the steep flow gradient at the airfoil surface and accurately determining lift, drag, and the separation of the flow from the blade surface. The average  $y^+$ , i.e., height of the first wall-adjacent cells inside the viscous sub layer of the boundary layer, was set to  $2 \times 10^{-5} c$ , which corresponds to  $y^+ \leq 1$ .

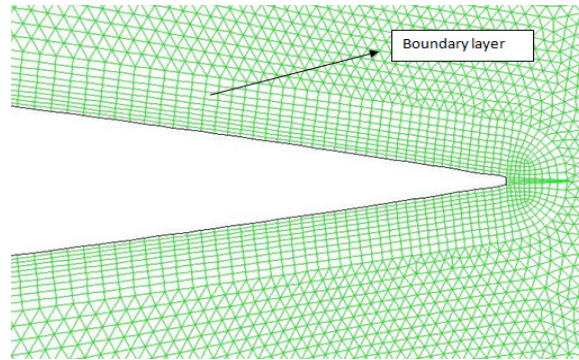


Figure 5. Boundary at the trailing edge of the airfoil

For the simulation, Fluent was employed, and a pressure-based segregated solver was chosen where the SIMPLE algorithm was used to handle the pressure-velocity coupling that exists. A 2nd-order special interpolation scheme for pressure was used, along with a 2nd-order upwind discretization scheme for the momentum equation and modified turbulent viscosity. The gradients required for the discretization of the convective, and diffusive fluxes were computed using a cell-based approach. Because the simulation was time dependent, a 2nd-order implicit time integration was chosen for the temporal discretization with a minimum convergence criteria were set to 1e-06. A time step was chosen small enough to reduce the number of iterations per time step and to properly model the transient phenomena. Turbulence modelling was accomplished through the use of the SST-k- $\omega$  turbulence model where a transport equation is solved for the eddy viscosity [17].

## Result and Discussions

In this section, the result of a baseline is presented first validated against the work of Paraschivoiu et al., followed by parametric studies on blade profiles, number of blades.

Figure 6 shows the coefficient of performance ( $C_p$ ) comparison between the qualitative accuracy of the algorithm compared with the reference turbine. The  $C_p$  was obtained from the ratio of the harnessed turbine power to the available wind power in the air. A good approximation of the turbine performance up to a TSR value of 5 can be observed, and slight over-estimation is observed beyond that value. It should be noted that the algorithm takes into account a varying interference factor in the function of the azimuth angle but does not consider the vertical variation of the free stream velocity. This explains the difference between the two results.

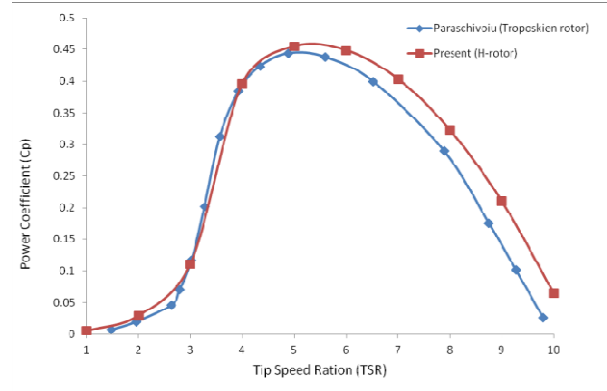


Figure 6. Comparison between DMST results and Paraschivoiu et al. [17]

Figure 7 shows the power coefficient ( $C_p$ ) comparison between computational fluid dynamic (CFD) and double multiple stream tube (DMST) model. The power coefficient from CFD analysis found from the data file is reported containing the dimensionless moment coefficient ( $C_m$ ) per unit length. The torque and power coefficient are calculated using equations 17 and 18.

$$C_T = \frac{T}{\frac{1}{2}\rho U^2 AR} \quad (17)$$

$$C_p = \frac{T\omega}{\frac{1}{2}\rho U^3 A} \quad (18)$$

where  $A$  and  $R$  are respectively the area of the turbine and the radius,  $C_T$  and  $C_p$  are the torque and power coefficient.

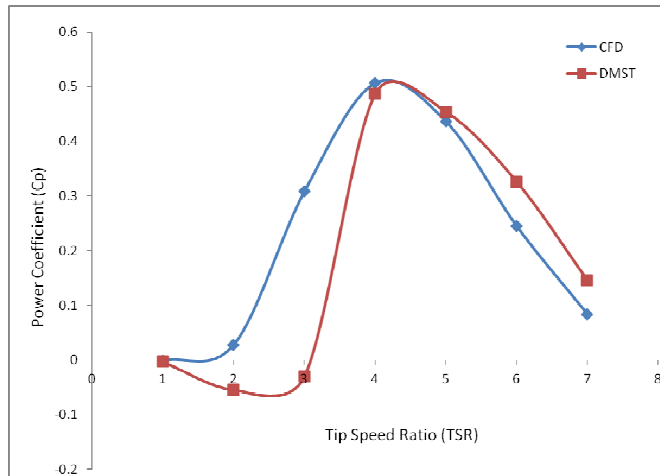


Figure 7. Power coefficient result for DMST and CFD

As can be seen, both CFD and DMST model Cp curves have shown minimum torque for lower tip speed ratios. The DMST model underestimates the CP value at lower tip speed ratio but predict higher CP value at higher tip speed ratio this agrees with [15].

### *Effect of Blade Profile*

The Darrieus VAWT has a positive angle of attack  $\alpha$  at the front side of the rotor and a negative angle  $\alpha$  at the backside, one has to use symmetrical airfoils. Three symmetric airfoils, NACA 0015, NACA 0018, NACA 0021, that are frequently used for Darrieus VAWT are examined in this study. These airfoils have lower maximum lift coefficients if they are compared to asymmetrical airfoils of the same thickness. To realize a certain lift, one must therefore use a larger chord.

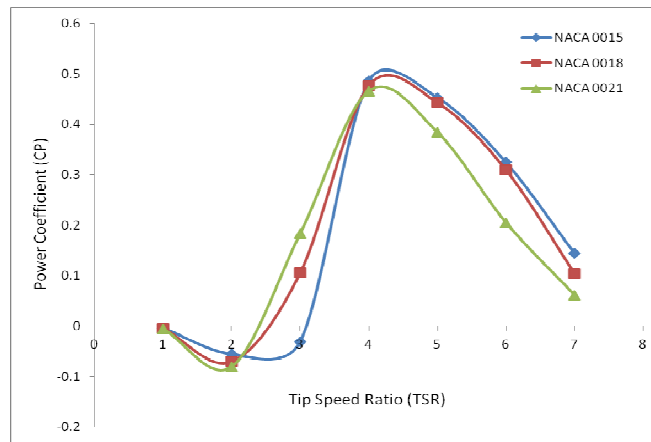


Figure 8. Power coefficient for the three airfoils

From Figure 8, it can be seen that the self-starting behavior is improved with thicker airfoils (NACA 0021). The maximum efficiency of NACA 0021 is around 0.4657 at TSR of 4,

however, beyond TSR 4, the performance of the thicker blade is penalized as far as efficiency is concerned. It can also be observed that the result of NACA 0015 and NACA 0018 are close to each other, but the NACA 0018 has better starting performance due to its thicker section.

### *Effect of Number of Blades*

Figure 9 represents the effect of blade number on the power coefficient as a function of the tip speed ratio. As can be observed, the peak of the power coefficient lowers with an increase in the number of blades. It can be said that larger number of blades reaches a maximum power coefficient for lower values of tip speed ratio but are not as efficient compared to three-bladed turbines. It can be said that larger number of blades improves starting performance of the turbine. For the two-bladed turbines, though they generate more power at high tip speed ratio, practically, the high rotational speed produces excessive vibration and consequently more noise and is less receptive for urban installation. A VAWT with larger number of blades achieves maximum power at TSR; however, more blades will eventually decrease the power coefficient.

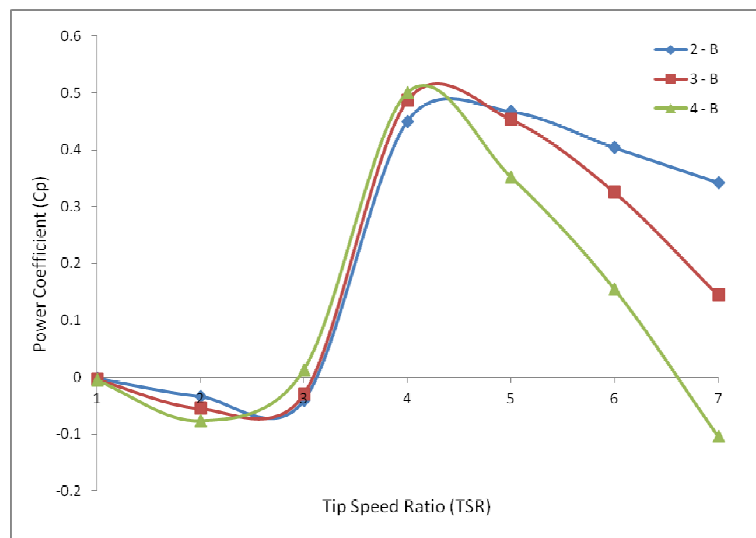


Figure 9. Power coefficient as a function of TSR for 2, 3 and 4-bladed rotor

Figure 10 shows the evolution of instantaneous torque coefficient of the 2-bladed, 3-bladed, and 4-bladed turbines at TSR of 3. As the number of blades increases, the torque coefficient decreases. In a complete 360° rotation of the turbine, the number of periods becomes higher as the number of blades increases, thereby creating a blockage effect and allowing less air to flow through the turbine. From CFD analysis, the contour of vorticity as shown in Figure 11 can be observed. This explains the decrease in the peak of the torque coefficient and power coefficient as the number of blade increases.

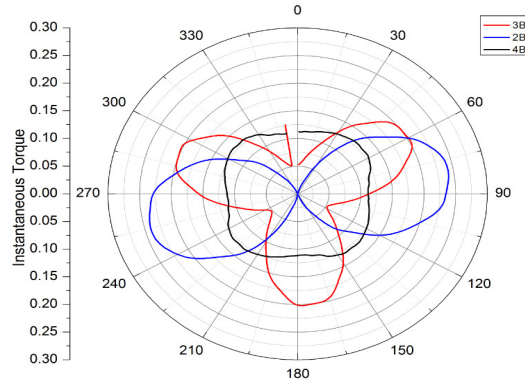


Figure 10. Instantaneous torque coefficient at TSR 3 for 2-, 3- and 4-bladed rotor

## Conclusion

A low-fidelity analysis tool based on double multiple stream model has been built using an extended airfoil database. It is validated using existing literature and a high-fidelity numerical simulation based on the Unsteady Reynolds Averaged Navier-Stoke equation. The results show that the double multiple stream tube model is not suitable for high solidity turbines. It is most suitable for low solidity wind turbines. The disadvantage is that low solidity turbines are not very applicable for a built in environment due to their large radius and the anticipated high rotational speed additional to associate noise. The  $C_p$  value obtained from DMST and CFD were compared shows that negative and/or minimum  $C_p$  and torque are generated at lower tip speed ratios, which implies that NACA 0015, NACA 0018, and NACA 0021 airfoils are not self-starting. Nevertheless, NACA0021 has shown to have better starting performance than the other two airfoils due to its thicker section. CFD results have shown to be more accurate and the flow physics, like vorticity, can be easily visualized. One major advantage of a low-fidelity analysis is that it can be used to determine an appropriate parameter for turbine performance before timely and expensive computation and experimentation.

## References

- [1] Aslam Bhutta, M. M., Hayat, N., Farooq, A. U., Ali, Z., Jamil, S. R. & Hussain, Z. (2012, May). Vertical Axis Wind Turbine—A Review of Various Configurations and Design Techniques. *Renewable and Sustainable Energy Review*, 16(4), 1926-1939.
- [2] Islam, M., Ting, D., & Fartaj, A. (2008, May). Aerodynamic Models for Darrieus-Type Straight-Bladed Vertical Axis Wind Turbines. *Renewable and Sustainable Energy Review*, 12(4), 1087-1109.
- [3] Paraschivoiu, I. (2002). *Wind Turbine Design: With Emphasis on Darrieus Concept*. Montreal: Presses Internationales Polytechnique.
- [4] Templin, R. J. (1974). *Aerodynamic Performance Theory for the NRC Vertical-Axis Wind Turbine*. Technical report #LTR-LA-160. Ottawa: National Research Council of Canada.

- [5] Strickland, J. H. (1975, October). *The Darrieus Turbine: A Performance Prediction Model Using Multiple Streamtubes*. Technical Report #SAND 75-0431. Albuquerque: Sandia National Laboratory.
- [6] Paraschivoiu, I. (1981, May). Double Multiple Streamtube Model for Darrieus in Turbines. *Lewis Research Center Wind Turbine Dynamics*, SEE N82-23684 14-44, 19-25.
- [7] Larsen, H. (1975). Summary of a Vortex Theory for the Cyclogiro. *Proceedings of the Second US National Conference on Wind Engineering Research*, V8-1-3.
- [8] Strickland, J., Webster, B., & Nguyen, T. (1979). A Vortex Model of the Darrieus Turbine: An Analytical and Experimental Study. *Journal of Fluid Engineering*, 5, 101-500.
- [9] Pawsey, N. C. K. (2002). *Development and Evaluation of Passive Variable-Pitch Vertical Axis Wind Turbines*. (Doctoral dissertation). University of New South Wales.
- [10] Dobrev, I., & Massouh, F. (2012, July). Exploring the Flow around a Savonius Wind Turbine. *16th International Symposium on Applications of Laser Techniques to Fluid Mechanics, 1996*, 1-9. Lisbon, Portugal.
- [11] Mohamed, M. H. (2012, November). Performance Investigation of H-Rotor Darrieus Turbine with New Airfoil Shapes. *Energy*, 47(1), 522-530.
- [12] Howell, R., Qin, N., Edwards, J., & Durrani, N. (2010, February). Wind Tunnel and Numerical Study of a Small Vertical Axis Wind Turbine. *Renewable Energy*, 35(2), 412-422.
- [13] Janajreh, I., Talab, I., & Macpherson, J. (2010). Numerical Simulation of Tower Rotor Interaction for Downwind Wind Turbine. *Modeling and Simulation in Engineering, 2010*, 1-11.
- [14] Yao, Z. Q. & Yang, C. L. (2013, February). Numerical Simulation of Unsteady Flow for Variable-Pitch Vertical Axis Wind Turbine. *Applied Mechanics and Materials, 291-294*, 490-495.
- [15] Castelli, M. R., Englaro, R., & Benini, E. A Proposal for a New Xfoil-Based Hybrid Extended Pole for Wind Turbine Applications. *Journal of Solar Energy Engineering*.
- [16] Paraschivoiu, I., Trifu, O., & Saeed, F. (2009). H-Darrieus Wind Turbine with Blade Pitch Control. *International Journal of Rotating Machinery*. Retrieved from <http://dx.doi.org/10.1155/2009/505343>
- [17] Salim, S. M. & Cheah, S. C. (2009). Wall  $y^+$  Strategy for Dealing with Wall-bounded Turbulent Flows. *Proceedings of the International MultiConference of Engineers and Computer Scientists, II*. Hong Kong.

## Biographies

FRANKLYN KANYAKO is currently a Ph.D. candidate at Masdar Institute in Abu Dhabi UAE. He is well-versed in wind turbine performance and analysis. His MS thesis work was on the development of low and high fidelity model for vertical wind turbine. Mr. Kanyako can be reached [fkanyako@masdar.ac.ae](mailto:fkanyako@masdar.ac.ae).

ISAM JANAJREH is currently an associate Mechanical Engineering professor and the director of the wind and waste to energy lab at the Masdar Institute. He is an internationally recognized expert in the area of multiphysics flow, wind energy and waste to energy particularly in the feedstock characterization thermochemical pathways, including gasification and pyrolysis. He has authored more than 80 publication in the subject and appeared in over 80 conferences. Dr. Isam Janajreh may be reached at [ijanajreh@masdar.ac.ae](mailto:ijanajreh@masdar.ac.ae).